HHS Public Access

Author manuscript

Proc SPIE Int Soc Opt Eng. Author manuscript; available in PMC 2016 March 20.

Published in final edited form as:

Proc SPIE Int Soc Opt Eng. 2016 February 13; 9692: . doi:10.1117/12.2218661.

Assessment of remineralized dentin lesions with thermal and near-infrared reflectance imaging

Robert C. Lee, **Cynthia L. Darling**, and **Daniel Fried***

University of California, San Francisco, San Francisco, CA 94143-0758

Abstract

Accurate detection and measurement of the highly mineralized surface layer that forms on caries lesions is important for the diagnosis of lesion activity. Previous studies have demonstrated that optical imaging methods can be used to measure the degree of remineralization on enamel lesions. The purpose of this study was to determine if thermal and near-IR reflectance imaging could be used to assess the remineralization process in simulated dentin lesions. Artificial bovine (n=15) dentin lesions were prepared by immersion in a demineralization solution for 24 hours and they were subsequently placed in an acidic remineralization solution for up to 12 days. The samples were dehydrated using an air spray for 30 seconds and imaged using thermal and InGaAs cameras. The area enclosed by the time-temperature curve, ΔQ, from thermal imaging decreased significantly with longer periods of remineralization. However, near-IR reflectance intensity differences, ΔI, before and after dehydration failed to show any significant relationship with the degree of remineralization. This study shows that thermal imaging can be used for the assessment of the remineralization of dentin lesions.

Keywords

Dentin; lesion activity; thermal imaging; near-IR imaging

1. INTRODUCTION

Sound dentin is more permeable to water than enamel due to the presence of dentinal tubules, which vary in size and density.[1] The capacity of water retention by the dentin lesion increases with the size and number of the enlarged dentinal tubules affected by demineralization.[2] Thus, the rate of water diffusion or the hydrodynamic properties of dentin may be used to estimate the state of mineralization and porosity of the exposed dentin surface.

The optical changes associated with water loss have been investigated via thermal imaging and near-IR imaging in enamel caries lesions.[3–5] In a previous study, we demonstrated that the rate of water evaporation from enamel could be analyzed for the assessment of remineralization.[6] The influence of hydration on dentin lesions can also be investigated as an indirect indicator of the decreased permeability of water due to remineralization. The

*daniel.fried@ucsf.edu.

objective of this work is to demonstrate that thermal and near-IR reflectance imaging can be used to monitor optical changes in simulated dentin lesions that have undergone remineralization during controlled dehydration.

2. MATERIALS AND METHODS

2.1. Sample preparation

Dentin blocks (n = 15), approximately 8–12 mm in length with a width of 2 mm and a thickness of 2 mm were prepared from extracted bovine incisors acquired from a slaughterhouse. The bovine enamel was removed from the outer surface towards the dentinoenamel junction (DEJ) exposing the dentin and the surfaces of the bovine dentin blocks were ground to a 9 μm finish. Each sample was partitioned into six regions or windows (1 sound control, 4 lesion and 1 remineralization control) by etching small incisions 1.8 mm apart across each of the dentin blocks using a laser. Incisions were etched using a transverse excited atmospheric pressure (TEA) CO_2 laser, an Impact 2500, GSI Lumonics (Rugby, UK), operating at 9.3 μm with a pulse duration of 15 μs, a pulse repetition rate of 200 Hz. A thin layer of acid-resistant varnish in the form of nail polish, Revlon (New York, NY), was applied to protect the sound and remineralization control windows before exposure to the demineralization solution. Samples with four exposed lesion windows were immersed in 45 mL aliquots of the demineralization solution for 24 hours. The demineralization solution, which was maintained at 37°C and pH 4.9, was composed of 2.0 mmol/L calcium, 2.0 mmol/L phosphate and 0.075 mol/L acetate. After the demineralization period, the acid resistant varnish was removed by immersion in acetone in an ultrasonic bath for 15 minutes and the acid-resistant varnish was applied again to the sound and lesion windows. Sample windows were subsequently exposed to an acidic remineralization solution for 4, 8 or 12-days by covering appropriate windows with acid resistant varnish at each time point. The acidic remineralization solution was composed of 4.1 mmol/L calcium, 15 mmol/L phosphate, 50 mmol/L lactic acid, 20 mmol/L HEPES buffer and 2 ppm F^- maintained at 37°C and a pH of 4.9. [7] The remineralization control window was exposed to the acidic remineralization solution for 12 days in order to examine its effect on sound dentin. After the 12 days of remineralization, the acid resistant varnish was removed and the samples were stored in 0.1 % thymol solution to prevent fungal and bacterial growth.

2.2. Dehydration setup

Each sample was placed in a mount connected to a high-speed XY-scanning motion controller system, Newport (Irvine, CA) ESP 300 controller and 850G-HS stages, coupled with an air nozzle and a light source. All surfaces excluding the windows were covered with black nail polish, OPI (North Hollywood, CA) in order to confine water loss to the exposed surface and prevent the transmission of light through the sides of the sample. Each sample was immersed in the water bath for 30 seconds while being vigorously shaken to enhance water diffusion. After the sample was removed from the water bath, an image was captured as an initial reference image and the air spray was activated. The air pressure was set to 15 psi and the computer controlled air nozzle was positioned 2 cm away from the sample. Each measurement consisted of capturing a sequence of images at 4 frames per second for 30

seconds. For each measurement, the air nozzle and the light source were centered on the ROI, and this process was repeated for each window (6 times per sample). The dehydration setup was completely automated using LabView™ software from National Instruments (Austin, TX).

2.3. Thermal Imaging and Analysis

An infrared (IR) thermography camera, Model A65 from FLIR Systems (Wilsonville, OR) sensitive from 7.5 – 13 μm with a resolution of 640 × 512 pixels, a thermal sensitivity of 50 mK and a lens with a 13 mm focal length was used to record temperature changes during the dehydration process. The ambient room temperature, flowing air temperature and water bath temperature were approximately 21 °C (294.15 K) and were consistent throughout the experiment. The object emissivity was set to 0.92, and the atmospheric temperature was set to 294.15 K.[8] Relative humidity was set at a default value of 50%; humidity values were not recorded, but every sample was measured under the same conditions. Previous studies have shown that ΔQ, the area enclosed by the time-temperature curve, can be used as a quantitative measure of porosity and can be used to discriminate between sound and demineralized enamel *in-vitro*.[3, 9]

Thermal images were processed and analyzed using a dedicated program written in Labview™. The thermography camera outputs a series of temperature measurements over time. Calibration was carried out via matching the measurements from the initial reference image to the ambient temperature. ΔQ was calculated and averaged over the 3 × 3 pixel ROI for each window.

2.4 Near-IR Reflectance Imaging and Analysis

An Indigo Alpha near-IR camera (FLIR Systems, Wilsonville, OR) with an InGaAs focal plane array, a spectral sensitivity range from 900 nm to 1750 nm, a resolution of 320 × 256 pixels and an InfiniMite™ lens (Infinity, Boulder, CO) was used to acquire all the images during the dehydration process. Light from a 150 W fiber-optic illuminator FOI-1 (E Licht Company, Denver, CO) was directed at the sample at an incident angle of approximately 60° in order to reduce specular reflection and the source to sample distance was fixed at 5 cm. Several band-pass (BP) and long-pass (LP) filters were used to provide different spectral distributions of near-IR light. Band-pass filters centered at 1300 nm with 90 nm bandwidth (1260–1340 nm), 1460 nm with 85 nm bandwidth (1420–1500 nm) from Spectrogon (Parsippany, NJ) and FEL LP series long-pass filters at 1400 nm (1400–1700 nm) and 1500 nm (1500–1700 nm) from Thorlabs (Newton, NJ) were used.

Near-IR reflectance images were processed and automatically analyzed using a dedicated program constructed with LabView™ software. A 5 × 5 pixel ROI was specified for each window and an average measurement was recorded for each time point. The intensity difference between the final and initial images, ΔI(t=30), was calculated using $I(t=30) - I_I$, where I(t=30) is the mean intensity at t = 30 seconds and I_I is the mean intensity prior to turning on the air nozzle.

2.5 Polarized Light Microscopy (PLM) and Transverse Microradiography (TMR)

After sample imaging was completed, 230 μm thick serial sections were cut using an Isomet 5000 saw (Buehler, IL), for PLM and TMR. PLM was carried out using a Model RZT microscope from Meiji Techno Co., LTD (Saitama, Japan) with an integrated digital camera, EOS Digital Rebel XT from Canon Inc. (Tokyo, Japan). The sample sections were imbibed in water and examined in the brightfield mode with crossed polarizers and a red I plate with 500 nm retardation. PLM images were acquired at 15× magnification.

A custom built digital microradiography (TMR) system was used to measure the volume percent mineral content in the areas of demineralization on the tooth sections.[10] High-resolution microradiographs were taken using Cu Kα radiation from a Philips 3100 X-ray generator and a Photonics Science FDI X-ray digital imager, Microphotonics (Allentown, PA). The X-ray digital imager consisted of a 1392×1040 pixel interline CCD directly bonded to a coherent micro fiber-optic coupler that transfers the light from an optimized gadolinium oxysulfide scintillator to the CCD sensor. The pixel resolution was 2.1 μm and the images were acquired at 10 frames per second. A high-speed motion control system with Newport UTM150 and 850G stages and an ESP 300 controller coupled to a video microscopy and a laser targeting system was used for precise positioning of the sample in the field of view of the imaging system.

3. RESULTS AND DISCUSSION

Figure 1 shows the visible (A), thermal (B) and near-infrared reflectance (C) images after exposure to remineralization, and the histological section images with PLM (D) and TMR (E) demonstrate that the lesion has been successfully remineralized over time. Windows exposed to the demineralization solution could not be easily discriminated from the sound and remineralization control windows by visual examination as shown in Fig. 1A.

ΔQ images calculated from the series of thermal imaging during 30 seconds of dehydration are shown in Fig. 1B and their time-temperature profiles are shown in Fig. 2A. Figure 2A shows that all line profiles exhibited the greatest temperature drop within the first 5 seconds of controlled dehydration and the lesion and sound windows manifest the slowest recovery to equilibrium. The magnitude of the temperature drop and the recovery time to equilibrium decreased with an increase in periods of exposure to the remineralization solution. There was also a significant reduction in ΔQ measurements after treatment with the remineralization solution and this suggests that there was a reduction in surface porosity and permeability that can be attributed to by the repair and occlusion of dentinal tubules due to the remineralization treatment.

ΔI images acquired from near-IR reflectance imaging with the 1400 nm long-pass filter during 30 seconds of dehydration are shown in Fig. 1C and their time-intensity difference profiles are shown in Fig. 2B. The intensity difference was recorded instead of raw intensity data due to differences in anatomical structure of the sample, i.e. variation in depth to pulp, presence of cracks, orientation and size of dentinal tubules and organic content of the tissue. ΔI measurements did not result in a significant difference between the lesion window and the windows that have been treated with the remineralization solution. In addition, images

taken with different filters had similar results with no significant differences. We speculate that the optical behavior of dentin at near-IR wavelength influenced the results of this study; sound dentin manifests higher scattering and absorption coefficients, almost an order of magnitude higher than enamel, due to the presence of dentinal tubules and the higher organic content.[11] Thermal imaging seems to be better suited for detecting remineralization in simulated dentin lesion samples. We plan to submit a full publication with the statistical analysis on all 15 samples in the future.

Acknowledgments

The authors acknowledge the support of NIH/NIDCR Grants F30-DE023278, R01-DE17869 and R01-DE14698.

REFERENCES

1. Prati C, Montebugnoli L, Suppa P, Valdrè G, Mongiorgi R. Permeability and morphology of dentin after erosion induced by acidic drinks. J. Periodontol. 2003; 74(4):428–436. [PubMed: 12747446]
2. Ozok AR, Wu MK, ten Cate JM, Wesselink PR. Effect of perfusion with water on demineralization of human dentin in vitro. J. Dent. Res. 2002; 81(11):733–737. [PubMed: 12407085]
3. Kaneko K, Matsuyama K, Nakashima S. Quantification of Early Carious Enamel Lesions by using an Infrared Camera. Early Detection of Dental Caries II, Annual Indiana Conference. 1999; 4:83–99.
4. Usenik P, Bürmen M, Fidler A, Pernus F, Likar B. Near-infrared hyperspectral imaging of water evaporation dynamics for early detection of incipient caries. J. Dent. 2014; 42(10):1242–1247. [PubMed: 25150104]
5. Ando M, Sharp N, Adams D. Pulse thermography for quantitative nondestructive evaluation of sound, de-mineralized and re-mineralized enamel. SPIE Proceeding. 2012; 8348S:1–7.
6. Lee RC, Darling CL, Fried D. Assessment of remineralization via measurement of dehydration rates with thermal and near-IR reflectance imaging. J. Dent. 2015; 43(8):1032–1042. [PubMed: 25862275]
7. Yamazaki H, Margolis HC. Enhanced enamel remineralization under acidic conditions in vitro. J. Dent. Res. 2008; 87(6):569–574. [PubMed: 18502967]
8. Lin M, Liu QD, Xu F, Bai BF, Lu TJ. In vitro investigation of heat transfer in human tooth. SPIE Proceeding. 2010; 7522N:1–7.
9. Zakian CM, Taylor AM, Ellwood RP, Pretty IA. Occlusal caries detection by using thermal imaging. J. Dent. 2010; 38(10):788–795. [PubMed: 20599464]
10. Darling CL, Featherstone JDB, Le CQ, Fried D. An automated digital microradiography system for assessing tooth demineralization. SPIE Proceeding. 2009; 7162T:1–7.
11. Chan AC, Darling CL, Chan KH, et al. Attenuation of near-IR light through dentin at wavelengths from 1300–1650-nm. SPIE Proceeding. 2014; 8929M:1–9.

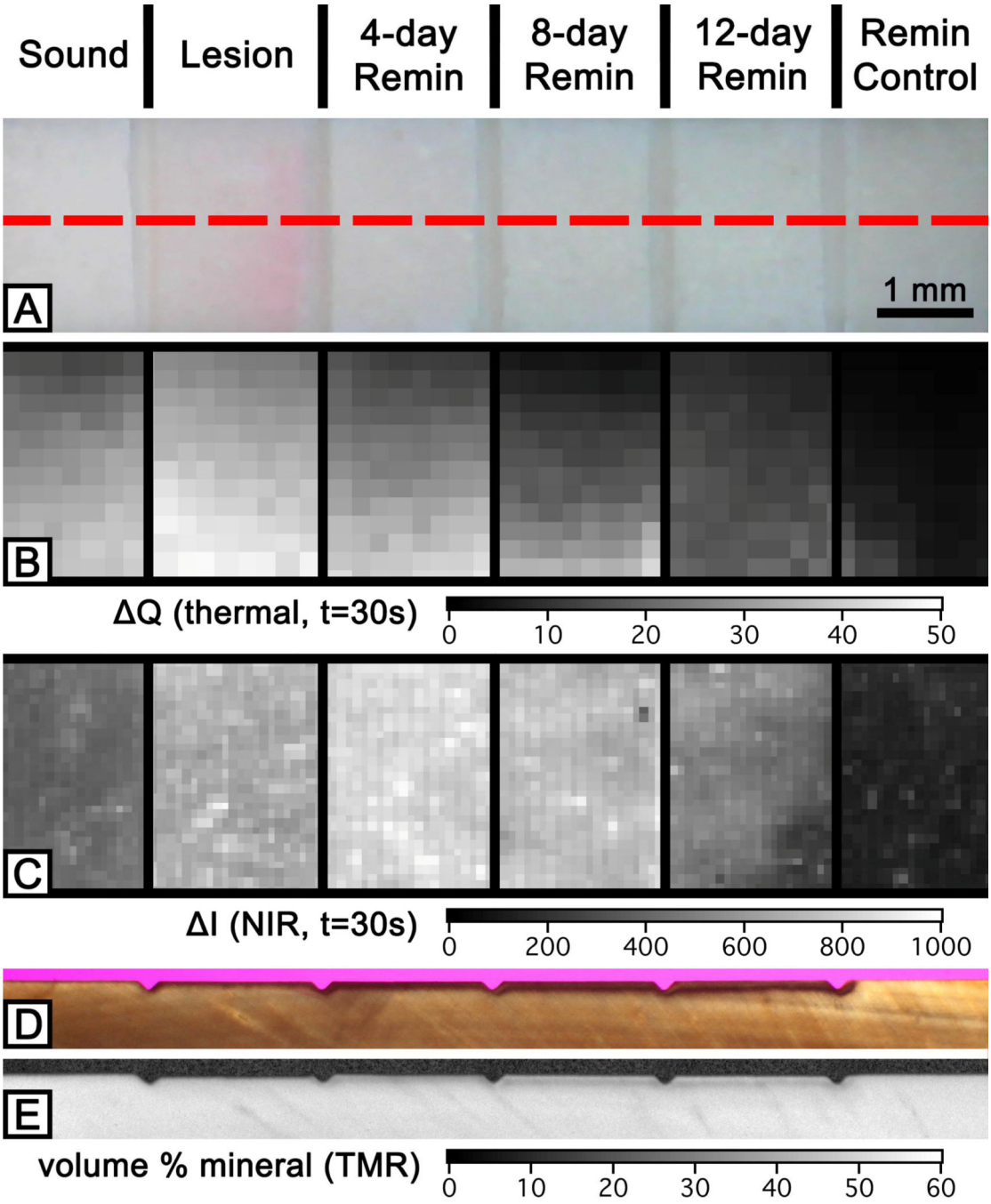

Fig. 1.

Visible (A), thermal (B) and near-infrared reflectance (C) imaging and histological PLM (D) and TMR (E) images of a sample. The red dotted line in the visible image (A) represents the position of section shown in (D) and (E). Near-infrared reflectance image (C) was taken with the 1400 nm long-pass filter.

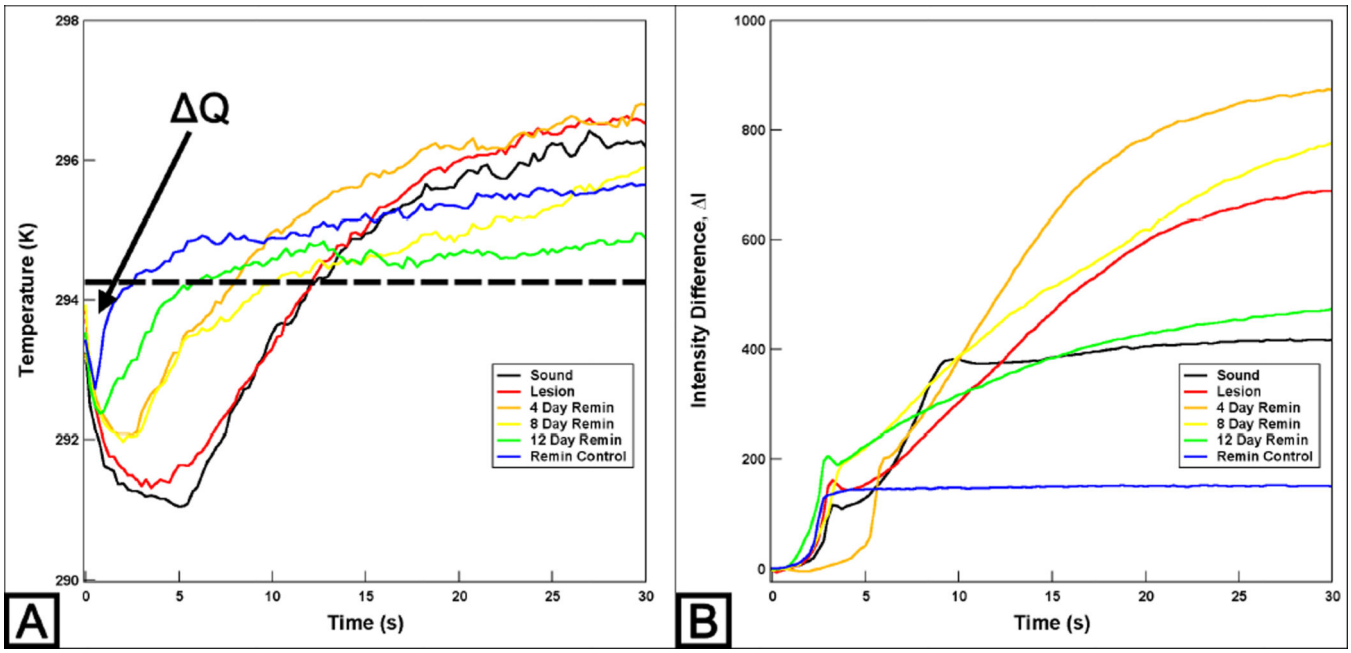

Fig. 2.

Typical time-temperature (A) and time-near-IR reflectance intensity difference (B) profiles over 30 seconds of the sample shown in Fig. 1. Dashed line (A) represents the initial temperature and ΔQ is the area under the dashed line enclosed by the time-temperature curve. Data with the 1400 nm long-pass filter is shown above (B).